Feasibility-Preserving ADMM Coordination of Transmission and Distribution Systems with Emergent Market Interface Equilibrium

Umar Salman, *Student member, IEEE*, Zongjie Wang*, *Senior member, IEEE*, Tongxin Zheng, *Fellow, IEEE*, Jinye Zhao, *Member, IEEE*, Chen Feng, *Student Member, IEEE*

***Abstract*—The growing penetration of distributed energy resources is transforming distribution systems into active participants in bulk power system operations, making coordinated transmission and distribution (T&D) optimization essential. However, most existing TSO–DSO coordination methods either impose explicit interface limits or treat physical feasibility and economic efficiency as separate design steps. To address this gap, this paper proposes a distributed coordination framework based on the alternating direction method of multipliers (ADMM) that simultaneously guarantees interface physical feasibility and yields market-consistent interface prices. First, the physically feasible interface power range for each DSO is explicitly computed via interface power optimization, and it is analytically shown that ADMM iterates and their convergence points remain strictly within these bounds without requiring additional interface constraints. Second, it is proven that the converged ADMM dual variables coincide with the marginal costs of interface power in the system Lagrangian and lie on the aggregated DSO bid curve, thus providing an emergent market equilibrium price signal at the TSO–DSO boundary. Simulation case studies on an enhanced IEEE 13-bus distribution feeder and a modified IEEE 39-bus transmission system integrated with three distribution networks (IEEE 33-, 69-, and 85-bus feeders) demonstrate the effectiveness and efficiency of the proposed method in coordinating T&D operations under 13–66% wind penetration, achieving up to 55% total cost reduction while maintaining DSO self-sufficiency levels between 57% and 100%.**

***Index Terms*—TSO-DSO coordination, ADMM, distributed optimization, interface pricing, physical feasibility, market equilibrium, cost minimization**

I. Introduction

The transformation of power systems driven by increasing levels of non-dispatchable energy resources (NDERs) has fundamentally altered the traditional hierarchical relationship between transmission and distribution networks [1], [2]. On the distribution side, the growing presence of distributed energy resources (DERs) is shifting distribution systems from passive load centers into active operational entities within the broader power system [3]. On the transmission side, large-scale variable energy resources (VERs) introduce additional uncertainty and operational variability. As a result, coordinated transmission and distribution (T&D) optimization has become essential for ensuring efficient and reliable system operation.

Traditional centralized optimization approaches struggle to meet these emerging needs due to computational complexity, information privacy concerns, and the requirement for autonomous operation of distribution systems [4]. As a result, distributed coordination frameworks have gained prominence because they allow T&D operators to solve local problems independently while exchanging limited information [5], [6]. However, despite the promise of distributed methods, several core challenges remain unresolved.

A central challenge is ensuring that distributed coordination intrinsically respects the physical feasibility of T&D interface power flows. Existing TSO–DSO coordination methods typically impose explicit interface limits or treat physical feasibility and economic efficiency as separate design steps [3], which obscures the underlying relationship between network constraints and the economic signals produced during coordination [7]. Although the alternating direction method of multipliers (ADMM) [5] has been widely adopted for distributed power system optimization, prior studies have not established a theoretical link between ADMM iterates and the physical interface feasibility bounds dictated by network constraints. Research on interface power management [8], [9] typically assumes predetermined limits or applies heuristic feasibility adjustments, leaving open the question of whether such feasibility can naturally arise from the ADMM structure itself. These unresolved issues highlight a fundamental gap: existing T&D coordination frameworks do not yet provide a unified treatment of physical feasibility, distributed computation, and economic interpretation.

To address these challenges, this paper develops a distributed T&D coordination framework based on the ADMM that establishes a direct theoretical coordination between ADMM updates, feasible interface power regions, and marginal-cost-based interface signals. The proposed framework first computes the physically feasible interface power range for each DSO using interface power optimization. It is then analytically demonstrated that ADMM iterates and their convergence points naturally remain within these feasibility bounds without requiring explicit interface constraints. Building on this property, the framework further shows that the converged ADMM dual variables coincide with the marginal cost of interface power in the system Lagrangian and lie on the aggregated DSO bid curve, thereby revealing that

U. Salman is with the Department of Electrical and Computer Engineering at the University of Connecticut, Storrs, CT, USA 06268. Z. Wang and C. Feng are with the Department of Electrical and Computer Engineering and Energy Institute at Colorado State University, Fort Collins, CO, USA 80526. T. Zheng and J. Zhao are with the Independent Systems Operator-New England (ISO-NE), Holyoke, MA, USA 01040. This research was funded in part by the ISO-NE project titled "Enabling Sustainable Coordination of Transmission and Distribution Systems Through Innovation Tools in Optimal System Dispatch." (*Corresponding author: Dr. Zongjie Wang, zongjie.wang@colostate.edu).

979-8-3315-8138-1

equilibrium-consistent interface signals emerge intrinsically from the distributed coordination process rather than from externally imposed mechanisms. The contributions of this paper include establishing the theoretical foundation integrating ADMM-based distributed coordination with physical interface feasibility, showing that equilibrium-consistent interface signals naturally emerge from the algorithm's dual updates, and validating these properties across diverse operating conditions in large-scale T&D systems.

II. Problem Formulation and Theoretical Framework

A. System Architecture

The coordinated T&D system comprises a transmission network operated by the TSO and K distribution networks managed by individual DSOs. The transmission system is characterized by the tuple $(\mathcal{T}^N, \mathcal{T}^L, \mathcal{T}^G, \mathcal{T}^W, \mathcal{T}^D)$, where $\mathcal{T}^N$ represents the set of transmission nodes, $\mathcal{T}^G \subseteq \mathcal{T}^N$ denotes controllable generators, $\mathcal{T}^W \subseteq \mathcal{T}^N$ represents VERs, $\mathcal{T}^L \subseteq \mathcal{T}^N \times \mathcal{T}^N$ defines transmission lines, and $\mathcal{T}^D \subseteq \mathcal{T}^N$ identifies boundary nodes connecting to distribution systems.

Each distribution system $k \in \mathcal{K} = \{1, 2, \ldots, K\}$ is represented by the tuple $(\mathcal{D}_k^N, \mathcal{D}_k^L, \mathcal{D}_k^G, \mathcal{D}_k^W)$, where $\mathcal{D}_k^N$ denotes the set of distribution nodes, $\mathcal{D}_k^G$ represents distributed generators, $\mathcal{D}_k^W$ indicates DERs, and $\mathcal{D}_k^L$ defines distribution lines. The distribution networks maintain radial topology with each node having a unique parent, except for the root node connecting to the transmission system. Let $\mathcal{T} = \{1, 2, \ldots, T\}$ denote the set of time periods in the optimization horizon.

B. Interface Power Optimization and Feasibility Bounds

Before presenting the ADMM coordination algorithm, the physical feasibility bounds of the T&D interface are first established via interface power optimization. For each DSO k at time t, the feasible interface power range is defined through the following optimization problems [9]:

$$P_{\min,k,t} = \min_{p_{im}} \; p_{im,k,t}, \tag{1a}$$

$$P_{\max,k,t} = \max_{p_{im}} \; p_{im,k,t}, \tag{1b}$$

$$\mathcal{F}_{k,t} = [\, P_{\min,k,t}, \; P_{\max,k,t} \,]. \tag{1c}$$

subject to DSO network constraints, generation limits, and power flow equations, (1a) defines the minimum interface power, the most negative feasible $p_{im,k,t}$, representing the maximum export capability of DSO k at time t. (1b) defines the maximum interface power, the most positive feasible $p_{im,k,t}$, representing the maximum import capability. Finally, (1c) expresses the feasible interface range $\mathcal{F}k, t$ as the interval bounded by these two extremes. With the convention $pim > 0$ for import and $p_{im} < 0$ for export. (1a)–(1c) explicitly captures both physical and operational limits governing power exchange between the TSO and DSO.

C. Cost Minimization Framework

The total system cost minimization problem is:

$$\min_{\mathbf{X},\mathbf{Y}} \quad \text{Cost}_{TS}(\mathbf{X}) + \sum_{k=1}^{K} \text{Cost}_{DS,k}(\mathbf{Y}_k), \tag{2}$$

subject to transmission network constraints, distribution network constraints, and the interface power balance constraint:

$$p_{ex,k,t} = p_{im,k,t}, \quad \forall k \in \mathcal{K}, \, t \in \mathcal{T}, \tag{3}$$

where $p_{ex,k,t}$ denotes the power exported from the TSO to DSO k at time t, and $p_{im,k,t}$ denotes the power imported by DSO k from the TSO at time t.

The TSO cost function incorporates generation costs, VER costs, demand utility, and interface payments:

$$\begin{aligned} \text{Cost}_{TS} = & \sum_{t \in \mathcal{T}} \Bigg[\sum_{g \in \mathcal{T}^G} C_g(p_{g,t}^{TS}) + \sum_{w \in \mathcal{T}^W} \pi_{R,w} \cdot w_{w,t}^{TS} \\ & - \sum_{d \in \mathcal{D}^{TS}} U_d(p_{d,t}) + \sum_{k \in \mathcal{K}} \beta_{k,t} \cdot p_{ex,k,t} \Bigg], \end{aligned} \tag{4}$$

where $C_g(\cdot)$ represents the generation cost function for generator g, $\pi_{R,w}$ denotes the VER cost per unit, $U_d(\cdot)$ is the demand utility function, and $\beta_{k,t}$ represents the interface price for power exchange at the TSO-DSO boundary.

Similarly, the DSO k cost function is:

$$\begin{aligned} \text{Cost}_{DS,k} = & \sum_{t \in \mathcal{T}} \Bigg[\sum_{g \in \mathcal{D}_k^G} C_{g,k}(p_{g,k,t}^{DS}) + \sum_{w \in \mathcal{D}_k^W} \pi_{R,w,k} \cdot w_{w,k,t}^{DS} \\ & - \sum_{d \in \mathcal{D}_k^N} U_{d,k}(p_{d,k,t}) - \beta_{k,t} \cdot p_{im,k,t} \Bigg], \end{aligned} \tag{5}$$

where the cost components are analogous to those in the TSO cost function. The interface price $\beta_{k,t}$ acts as a transfer payment between TSO and DSO, ensuring revenue neutrality across the interface.

D. TSO Optimization Problem

The TSO solves the following optimization problem:

$$\begin{aligned} \min_{\mathbf{X}^{TS}} \quad & \sum_{t \in \mathcal{T}} \Bigg[\sum_{g \in \mathcal{T}^G} \left(c_{g,2}(p_{g,t}^{TS})^2 + c_{g,1} p_{g,t}^{TS} + c_{g,0} u_{g,t} \right) \\ & + \sum_{w \in \mathcal{T}^W} \pi_{R,w} w_{w,t}^{TS} + \sum_{k \in \mathcal{K}} \beta_{k,t} p_{ex,k,t} \Bigg], \end{aligned} \tag{6}$$

subject to the following transmission network constraints:

Power balance at each node $i \in \mathcal{T}^N$ and time $t \in \mathcal{T}$:

$$\sum_{g \in \mathcal{G}_i} p_{g,t}^{TS} + \sum_{w \in \mathcal{W}_i} w_{w,t}^{TS} - d_{i,t}^{TS} = \sum_{j \in \mathcal{N}_i} B_{ij}(\theta_{i,t} - \theta_{j,t}), \tag{7}$$

where $d_{i,t}^{TS}$ represents the demand at node i, B_{ij} is the susceptance of the transmission line between nodes i and j, $\theta_{i,t}$ is the voltage angle at node i, and $\mathcal{N}_i$ denotes the set of nodes adjacent to node i.

979-8-3315-8138-1

Generator capacity constraints:

$$u_{g,t} \cdot P_g^{\min} \leq p_{g,t}^{TS} \leq u_{g,t} \cdot P_g^{\max}, \quad \forall g \in \mathcal{T}^G, t \in \mathcal{T}, \tag{8}$$

where $u_{g,t}$ is the binary commitment status, and $P_g^{\min}$ and $P_g^{\max}$ are minimum and maximum generation limits.

Ramping constraints:

$$-R_g^{\text{down}} \leq p_{g,t}^{TS} - p_{g,t-1}^{TS} \leq R_g^{\text{up}}, \quad \forall g \in \mathcal{T}^G, t \in \mathcal{T}, \tag{9}$$

where R_g^{up} and R_g^{down} denote the upward and downward ramping rates.

Line flow limits:

$$|B_{ij}(\theta_{i,t} - \theta_{j,t})| \leq F_{ij}^{\max}, \quad \forall (i,j) \in \mathcal{T}^L, t \in \mathcal{T}, \tag{10}$$

where $F_{ij}^{\max}$ is maximum thermal limit of transmission line.

E. DSO Optimization Problem

Each DSO k solves the following cost minimization problem:

$$\min_{\mathbf{Y}_k^{DS}} \quad \sum_{t \in \mathcal{T}} \Bigg[\sum_{g \in \mathcal{D}_k^G} C_{g,k}(p_{g,k,t}^{DS}) + \sum_{w \in \mathcal{D}_k^W} \pi_{R,w,k} w_{w,k,t}^{DS} - \beta_{k,t} p_{im,k,t} \Bigg], \tag{11}$$

subject to distribution network constraints using SOCP relaxation.

Power balance equations for real and reactive power at each node $i \in \mathcal{D}_k^N$ and time $t \in \mathcal{T}$:

$$p_{g,i,t} + p_{w,i,t} - d_{i,t} + \sum_{j \in \mathcal{C}_i} (P_{ji,t} - r_{ji} l_{ji,t}) = \sum_{j \in \mathcal{C}_i} P_{ij,t}, \tag{12}$$

$$q_{g,i,t} + q_{w,i,t} - q_{d,i,t} + \sum_{j \in \mathcal{C}_i} (Q_{ji,t} - x_{ji} l_{ji,t}) = \sum_{j \in \mathcal{C}_i} Q_{ij,t}, \tag{13}$$

where $P_{ij,t}$ and $Q_{ij,t}$ denote real and reactive power flows on line (i,j), r_{ji} and x_{ji} are line resistance and reactance, $l_{ji,t}$ is the squared current magnitude, and $\mathcal{C}_i$ represents the set of child nodes of node i in the radial distribution network.

Voltage relationship incorporating SOCP relaxation:

$$v_{j,t} = v_{i,t} - 2(r_{ij} P_{ij,t} + x_{ij} Q_{ij,t}) + (r_{ij}^2 + x_{ij}^2) l_{ij,t}, \quad \forall (i,j) \in \mathcal{D}_k^L, \tag{14}$$

where $v_{i,t}$ represents squared voltage magnitude at node i.

Current magnitude constraint (second-order cone relaxation):

$$l_{ij,t} \geq \frac{P_{ij,t}^2 + Q_{ij,t}^2}{v_{i,t}}, \quad \forall (i,j) \in \mathcal{D}_k^L, t \in \mathcal{T}, \tag{15}$$

Voltage limits:

$$V_{\min}^2 \leq v_{i,t} \leq V_{\max}^2, \quad \forall i \in \mathcal{D}_k^N, t \in \mathcal{T}, \tag{16}$$

where $V_{\min}$ and $V_{\max}$ are the minimum and maximum allowable voltage magnitudes.

F. ADMM Coordination Algorithm

The ADMM algorithm coordinates the TSO and DSO problems through iterative updates of primal and dual variables [5], [10]. At iteration ν, the algorithm proceeds as follows:

TSO Problem: The TSO solves its optimization problem with fixed dual variables:

$$\mathbf{X}^{TS,(\nu+1)} = \arg\min_{\mathbf{X}^{TS}} \quad \text{Cost}_{TS}(\mathbf{X}^{TS}) + \sum_{k,t} \mu_{k,t}^{(\nu)} p_{ex,k,t} + \frac{\rho}{2} \sum_{k,t} (p_{ex,k,t} - p_{im,k,t}^{(\nu)})^2, \tag{17}$$

where $\mu_{k,t}^{(\nu)}$ is the dual variable (Lagrange multiplier) at iteration ν and $\rho > 0$ is the augmented Lagrangian penalty parameter.

DSO Problems: Each DSO k independently solves:

$$\mathbf{Y}_k^{DS,(\nu+1)} = \arg\min_{\mathbf{Y}_k^{DS}} \quad \text{Cost}_{DS,k}(\mathbf{Y}_k^{DS}) - \sum_{t} \mu_{k,t}^{(\nu)} p_{im,k,t} + \frac{\rho}{2} \sum_{t} (p_{im,k,t} - p_{ex,k,t}^{(\nu+1)})^2, \tag{18}$$

with the constraint that $p_{im,k,t}^{(\nu+1)} \in \mathcal{F}_{k,t}$. Note that the DSO explicitly enforces the bounds in (1c), while (18) ensures that the TSO also respects them at optimality via the ADMM coordination mechanism. **Dual Update**: Update the dual variables (interface prices):

$$\mu_{k,t}^{(\nu+1)} = \mu_{k,t}^{(\nu)} + \rho(p_{ex,k,t}^{(\nu+1)} - p_{im,k,t}^{(\nu+1)}). \tag{19}$$

The algorithm converges when the primal residual $r^{(\nu)} = \|p_{ex}^{(\nu)} - p_{im}^{(\nu)}\|$ and dual residual $s^{(\nu)} = \|\rho(p_{im}^{(\nu)} - p_{im}^{(\nu-1)})\|$ fall below prescribed tolerances [5].

At convergence, the interface price emerges as $\beta_{k,t} = \mu_{k,t}^*$, representing the marginal cost of power transfer at the TSO-DSO interface. This price signal ensures efficient resource allocation across system boundaries without requiring centralized coordination or bilateral negotiations.

G. Theoretical Results

1) Theorem 1: Feasibility Preservation: Let $[P_{\min,k,t}, P_{\max,k,t}]$ be the feasible interface power range for DSO k at time t. Then the ADMM solution satisfies:

$$p_{ex,k,t}^* = p_{im,k,t}^* \in [P_{\min,k,t}, P_{\max,k,t}], \quad \forall k \in \mathcal{K}, t \in \mathcal{T}. \tag{20}$$

Proof: At each ADMM iteration ν, the DSO solves:

$$p_{im,k,t}^{(\nu+1)} \in \arg\min_{p \in \mathcal{F}_{k,t}} \Big\{ \text{Cost}_{DS,k}(p) - \mu_{k,t}^{(\nu)} p + \frac{\rho}{2}(p - p_{ex,k,t}^{(\nu)})^2 \Big\}. \tag{21}$$

Since $\mathcal{F}_{k,t}$ is compact and convex, the solution exists and satisfies $p_{im,k,t}^{(\nu+1)} \in \mathcal{F}_{k,t}$ by definition of the optimization domain. Since each iterate maintains feasibility, and ADMM convergence respects the feasible set of the constituent subproblems, at convergence we have $p^*_{ex,k,t} = p^*_{im,k,t} \in \mathcal{F}_{k,t}$.

2) Theorem 2: Price-Marginal Cost Equivalence: The converged ADMM dual variable equals the marginal cost of interface power in the system Lagrangian:

$$\mu^*_{k,t} = \frac{\partial \mathcal{L}_{\text{system}}}{\partial p_{\text{interface}}}\bigg|_{p=p^*}, \tag{22}$$

where $\mathcal{L}_{system}$ is the augmented Lagrangian of the overall coordination problem.

Proof: At optimality, the KKT conditions of the coordinated problem yield:

$$\nabla_p \text{Cost}_{TS}(p^*_{ex}) + \mu^* = 0, \tag{23}$$

$$\nabla_p \text{Cost}_{DS}(p^*_{im}) - \mu^* = 0. \tag{24}$$

Combined with the convergence condition $p^*_{ex} = p^*_{im} = p^*$, these equations imply:

$$\mu^* = -\nabla_p \text{Cost}_{TS}(p^*) = \nabla_p \text{Cost}_{DS}(p^*), \tag{25}$$

which represents the marginal value of interface power in both the TSO and DSO optimization problems, confirming the economic interpretation of the dual variable.

3) Theorem 3: Market Equilibrium Correspondence: The ADMM solution (p^*, μ^*) lies on the aggregated bid curve constructed from DSO cost functions at the point where TSO supply marginal cost equals DSO demand marginal utility:

$$\mu^* = \text{BidCurve}(p^*) = \frac{\partial \text{Cost}_{DS}}{\partial p_{im}}\bigg|_{p_{im}=p^*}. \tag{26}$$

This establishes that ADMM finds the market equilibrium point where TSO supply marginal cost meets DSO demand marginal utility.

III. Simulation Results and Validation

The proposed framework was evaluated using two system configurations. The first configuration assessed the feasible interface region using a single DSO test network derived from the enhanced IEEE 13-bus distribution feeder. This system preserves the original radial topology with 13 buses and 12 lines and incorporates a representative mix of DERs, including solar and wind units, energy storage, and flexible demand response capabilities. The full T&D coordination was subsequently tested on a larger integrated system consisting of a modified IEEE 39-bus transmission interconnected with three distribution systems, providing a comprehensive setting to examine coordination behavior under more complex operating conditions. The distribution systems consist of the IEEE 33-bus (DS1), IEEE 69-bus (DS2), and IEEE 85-bus (DS3) feeders, connected to the transmission at buses 3, 10, and 17, respectively, via tie-lines rated at 1000 MW and 2000 MVAr.

Four scenarios were evaluated to assess system performance under varying NDER and load conditions. The Baseline case represents moderate wind penetration and balanced power exchange between TSO and DSOs. The High NDER case increases wind generation and DSO self-sufficiency, resulting in limited interface trading. The Balanced Penetration case achieves higher NDER integration with stable interface flows, while the Wind-Dominant case tests the framework under extreme wind penetration, highlighting system behavior under high variability and export conditions.

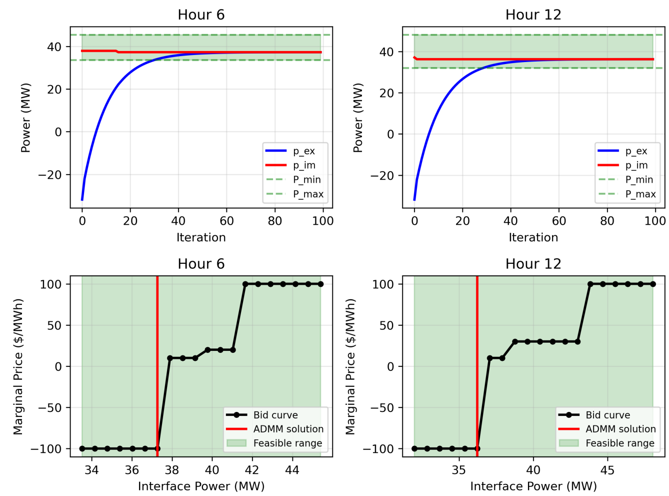

Fig. 1. ADMM power exchange convergence within interface power optimization bounds for hour 6 and hour 12. Top row shows convergence trajectories with feasible range (green shaded area). Bottom row displays corresponding bid curves with ADMM equilibrium points (red lines) and interface prices (green dotted lines).

A. ADMM Convergence Within Physical Bounds

The results between the ADMM convergence within physical bounds are first analyzed. Fig. 1 presents the empirical validation of Theorem 1, showing ADMM convergence behavior relative to physical feasibility bounds across four representative hours. It observes that all ADMM trajectories for TSO exports and DSO imports converge within the green-shaded feasible region without explicit constraints, demonstrating guaranteed feasibility. The algorithm achieves rapid convergence within 40–60 iterations even when initialized far from the feasible bounds. At convergence, interface prices align with the marginal costs on the bid curves, confirming accurate price formation, while the final solutions consistently settle near the economic optimum rather than at boundary extremes, reflecting efficient market coordination.

Fig. 2 illustrates the intrinsic coordination between ADMM convergence and physical feasibility across all test hours. The figure shows that all ADMM solutions remain strictly within the feasible interface range, demonstrating the algorithm's consistency with network limits.

B. Economic Performance Analysis

The results from the second case study are further discussed. Tab. I summarizes the economic performance across all scenarios, revealing substantial cost variations driven by the generation mix and the effectiveness of T&D coordination.

The total system cost decreases substantially across the four scenarios, from \$1.31 million in Scenario 1 to \$0.58 million in

979-8-3315-8138-1

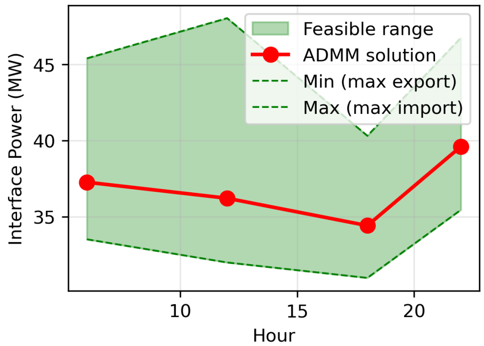

Fig. 2. A comprehensive relationship analysis shows that ADMM solutions remain within the interface power optimization bounds across all 24 hours.

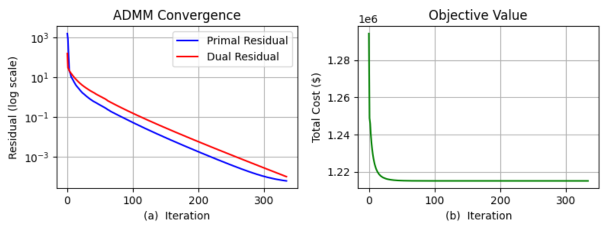

Fig. 3. Integrated ADMM convergence and system coordination analysis for Scenario 1: (a) Convergence residuals, (b) Objective evolution, (c) Interface power exchanges, (d) Marginal prices (LMPs), (e) TSO generation dispatch, and (f) DSO import profiles.

Scenario 4, representing a 55% reduction enabled by increased utilization of non-dispatchable energy resources. The cost per MWh likewise declines from \$4.81 to \$2.15, indicating that coordinated T&D operation effectively captures the economic value of higher VER penetration. Interface trading volumes further illustrate the coordination dynamics: Scenario 1 shows moderate exports from the transmission system (40 GWh), Scenario 2 exhibits minimal trading (18.6 GWh) due to high DSO self-sufficiency, Scenario 3 reflects balanced exchanges (31 GWh), and Scenario 4 produces the highest trading level (56 GWh) as surplus wind generation is efficiently redistributed. Interface prices follow the underlying supply conditions, with Scenarios 1 and 3 maintaining mid-range values (approximately \$9.40–\$9.46/MWh), Scenario 2 showing higher prices (\$11.01/MWh) under resource scarcity, and Scenario 4 reaching the lowest prices (\$5.87/MWh) during significant VER abundance. Together, these results demonstrate that the proposed coordination framework effectively aligns interface power flows and economic signals with system conditions. Fig. 3 further illustrates the ADMM coordination process under Scenario 1, where the primal and dual residuals in Fig. 3(a) decrease rapidly from the order of 10^3 to below 10^{-5}, indicating strong numerical convergence and tight synchronization between the TSO and DSO subproblems. The total system cost in Fig. 3(b) stabilizes near \$1.26 million within the first 100 iterations, confirming fast convergence and economic efficiency.

TABLE I
ECONOMIC PERFORMANCE SUMMARY ACROSS ALL SCENARIOS.

Metric	Sce. 1	Sce. 2	Sce. 3	Sce. 4
Total Cost (\$M)	1.31	1.05	0.92	0.58
Cost per MWh (\$/MWh)	4.81	5.32	3.86	2.15
Wind Penetration (%)	13.25	22.4	36.28	65.77
Interface Trading (GWh)	40.0	18.6	31.0	56.0
Avg. Interface Price (\$/MWh)	9.46	11.01	9.40	5.87
ADMM Iterations	240	329	195	30

IV. CONCLUSION

This paper presented a comprehensive distributed coordination framework for TSO–DSO systems using the alternating direction method of multipliers, supported by theoretical foundations. The proposed cost minimization framework enables coordinated transmission and distribution operations while preserving operator autonomy and information privacy. The study established three key theoretical results: ADMM convergence naturally satisfies physical interface feasibility bounds without requiring explicit constraints; the dual variables at convergence correspond to true marginal costs on the aggregated bid curves; and the framework intrinsically unifies the physical and economic characteristics of coordinated T&D operation through its mathematical structure. These contributions advance the fundamental understanding of distributed optimization in large-scale power systems. Future research may extend this framework to multi-period uncertainty modeling, stochastic NDER variability, and real-time T&D operations.

REFERENCES

[1] X. Xiao, F. Wang, M. Shahidehpour, Z. Li, and M. Yan, "Coordination of distribution network reinforcement and der planning in competitive market," *IEEE Transactions on Smart Grid*, vol. 12, no. 3, pp. 2261–2271, 2020.

[2] A. G. Givisiez, K. Petrou, L. F. Ochoa, and P. H. Nardelli, "A review on tso-dso coordination models and solution techniques," *Electric Power Systems Research*, vol. 189, p. 106659, 2020.

[3] S. D. Manshadi and M. E. Khodayar, "A hierarchical electricity market structure for the smart grid paradigm," *IEEE Transactions on Smart Grid*, vol. 7, no. 4, pp. 1866–1875, 2015.

[4] D. K. Molzahn, F. Dörfler, H. Sandberg, S. H. Low, S. Chakrabarti, R. Baldick, and J. Lavaei, "A survey of distributed optimization and control algorithms for electric power systems," *IEEE Transactions on Smart Grid*, vol. 8, no. 6, pp. 2941–2962, 2017.

[5] S. Boyd, N. Parikh, E. Chu, B. Peleato, and J. Eckstein, "Distributed optimization and statistical learning via the alternating direction method of multipliers," *Foundations and Trends in Machine Learning*, vol. 3, no. 1, pp. 1–122, 2011.

[6] U. T. Salman, Z. Wang, and T. M. Hansen, "Optimizing grid resilience: A capacity reserve market for high impact low probability events," in *2024 IEEE Power & Energy Society General Meeting (PESGM)*. IEEE, 2024, pp. 1–5.

[7] M. C. Caramanis, E. Ntakou, W. W. Hogan, A. Chakrabortty, and J. Schoene, "Co-optimization of power and reserves in dynamic t&d power markets with nondispatchable renewable generation and distributed energy resources," *Proceedings of the IEEE*, vol. 104, no. 4, pp. 807–836, 2016.

[8] S. Huang, Q. Wu, C. Huang, and Z. Wang, "Adaptive admm for distributed optimal power flow problem with renewable energy," *IEEE Transactions on Industrial Informatics*, vol. 16, no. 3, pp. 1711–1721, 2019.

[9] F. Capitanescu, "Computing cost curves of active distribution grids aggregated flexibility for tso-dso coordination," *IEEE Transactions on Power Systems*, vol. 39, no. 1, pp. 2381–2384, 2023.

[10] T. Chen, Y. Sun, and W. Yin, "Alternating direction method of multipliers for machine learning," *IEEE Transactions on Pattern Analysis and Machine Intelligence*, vol. 44, no. 12, pp. 9612–9634, 2022.

979-8-3315-8138-1